4096-element continuous face-sheet MEMS deformable mirror for high-contrast imaging

Steven A. Cornelissen
Paul A. Bierden
Boston Micromachines Corporation
30 Spinelli Place
Cambridge, Massachusetts 02138
E-mail: sac@bostonmicromachines.com

Thomas G. Bifano
Boston Micromachines Corporation
30 Spinelli Place
Cambridge, Massachusetts 02138
and
Boston University Photonics Center
8 Saint Mary's Street
Boston, Massachusetts 02215

Charlie V. Lam
Boston Micromachines Corporation
30 Spinelli Place
Cambridge, Massachusetts 02138

Abstract. We present the progress in the development of a 4096-element microelectromechanical systems (MEMS) deformable mirror, fabricated using polysilicon surface micromachining manufacturing processes, with 4 μm of stroke, a surface finish of <10 nm rms, a fill factor of 99.5%, and a bandwidth of >5 kHz. The packaging and high-speed drive electronics for this device, capable of frame rates of 22 kHz, are also presented. © *2009 Society of Photo-Optical Instrumentation Engineers.* [DOI: 10.1117/1.3158067]

Subject terms: deformable mirror; MEMS; adaptive optics; wavefront correction; MEMS packaging; MEMS characterization.

Paper 09043SSPR received Mar. 9, 2009; revised manuscript received Apr. 28, 2009; accepted for publication Apr. 30, 2009; published online Jul. 29, 2009. This paper is a revision of a paper that appeared at the SPIE conference MEMS Adaptive Optics II, January 2008, San Jose, California. The paper presented there appears (unrefereed) in SPIE Proceedings Vol. 6888.

1 Introduction

A 4096 element continuous face-sheet deformable mirror system is being developed for the Gemini Planet Imaging instrument, for high-order wavefront aberrations correction to achieve contrast ratios of 10^7–10^8 required to directly detect Jupiter-like planets outside of our solar system that are a billion times fainter than the sun and obscured by light from their parent star, atmospheric aberrations, and optical imperfections in the imaging system.[1] The deformable mirror (DM) design and fabrication is based on a commercially available, 1024 element microelectromechanical systems (MEMS) DM that has been demonstrated to be capable of flattening a wavefront 0.54 nm rms within the active control band (12.8 nm rms total), in a high-contrast imaging testbed using a 13-bit, closed-loop control system.[2] To achieve the desired performance for the Gemini Planet Imager, this DM design is being extended to 4096 elements with 4 μm of mechanical stroke, a surface figure better than 10 nm rms, and a bandwidth of 5 kHz. The DM is mounted and wire bonded in a ceramic carrier to provide structural support on electrical interconnections. Eight high-density flex cables connect the DM to the drive electronics, which provides 4096 channels of parallel, high-voltage signals to allow control of each individual DM actuator with 14-bit precision.

2 Deformable Mirror Architecture

MEMS deformable mirrors produced by Boston Micromachines Corporation (BMC) are based on the surface-micromachined, poly-silicon double cantilever actuator architecture pioneered at Boston University,[3,4] illustrated in Fig. 1. The device structure consists of actuator electrodes underneath a double cantilever flexure that is electrically isolated from the electrodes and maintained at a ground potential. The actuators are arranged in a 64×64 grid, on a pitch of 400 μm, and the flexible mirror surface is connected to the center of each actuator through a small attachment post that translates the actuator motion to a mirror surface deformation.

This MEMS DM architecture allows for local deformation of the mirror membrane with an influence function of 26–32% on its nearest neighbor. Figure 2 shows wavefront measurements generated using a 140 element, 2.5 μm stroke, BMC MEMS DM in a closed-loop system, demonstrating the ability of the DM to take the shape of high-order Zernike terms.

Element deflection is achieved using electrostatic actuators that perform without hysteresis. As illustrated in Fig. 3, the actuator consists of a double cantilever flexure and the fixed electrode, separated by gap, g. An attractive electrostatic force results when a potential difference is applied across this gap, resulting in a downward deflection of the actuator flexure. The electrostatic force is counteracted by the mechanical restoring force of the flexure that provides stable and repeatable actuator control. Using shaped electrodes and perforated double cantilever flexure designs the stable operating range can be extended to over 50% of the surface normal gap to minimize drive voltages and ease manufacturability.

3 4096 Element MEMS DM Design

A 68×68 element actuator array, supporting a 26.8-mm mirror face sheet is located in the center of a 49-mm single-

1932-5150/2009/$25.00 © 2009 SPIE

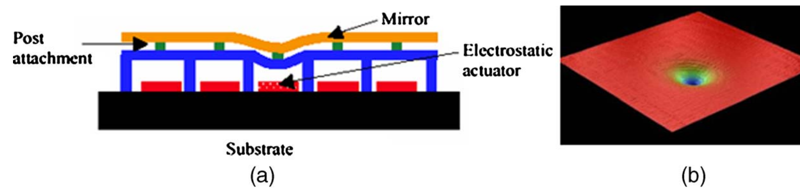

Fig. 1 (a) Illustration of a crosssection of 1×5 electrostatically actuated MEMS deformable mirror. (b) Optical profiler measurement of mirror surface figure of a continuous face-sheet BMC DM resulting from actuation of a single element. The influence of the single-element deflection only affects its immediate neighbors leaving the rest of the mirror surface unchanged.

crystal silicon die, as shown in Fig. 4. Although the active aperture is 64×64 elements, two rows of elements are used around the periphery of the active area to eliminate edge affects caused by thin-film stresses that result in actuator performance variations; adding these dummy elements makes the performance of all the 4096 element uniform. The additional rows also reduce optical edge effects resulting from the CMP processes, which induce a rounding of the edge elements that may not be compensated for using the DM actuators. Small holes, 18 per element, are etched in the mirror face sheet and yield a fill factor of $\sim$99.5%. The small holes are required for device manufacturing and to control squeeze film damping that affects the dynamic response of the device. Polysilicon wire traces are routed to four rows of bond pads around the periphery of the die.

The device performance goals to enable high-contrast imaging in the Gemini Planet Imager instrument are listed in Table 1.

4 MEMS DM Fabrication Process

The 4096 element DM is fabricated using surface micromachining batch-fabrication techniques. The custom fabrication process, illustrated in Fig. 5, uses four layers of polysilicon (poly) alternating with dielectric films and two sacrificial layers of phosphosilicate glass. For batch processing, 150-mm-diam silicon wafers are used as substrates. A low-stress silicon nitride layer is deposited, lithographically patterned, and etched to allow electrical access to the substrate. The first layer of poly-silicon is deposited, patterned, and etched to create the wire routing for the array. This is followed by the deposition of a silicon nitride film that electrically isolates the electrical wiring layer. Small vias are etched in the dielectric film to allow interconnections to each wire. A second polysilicon film is deposited, patterned, and etched to form the actuator electrodes. To define the surface normal gap between the

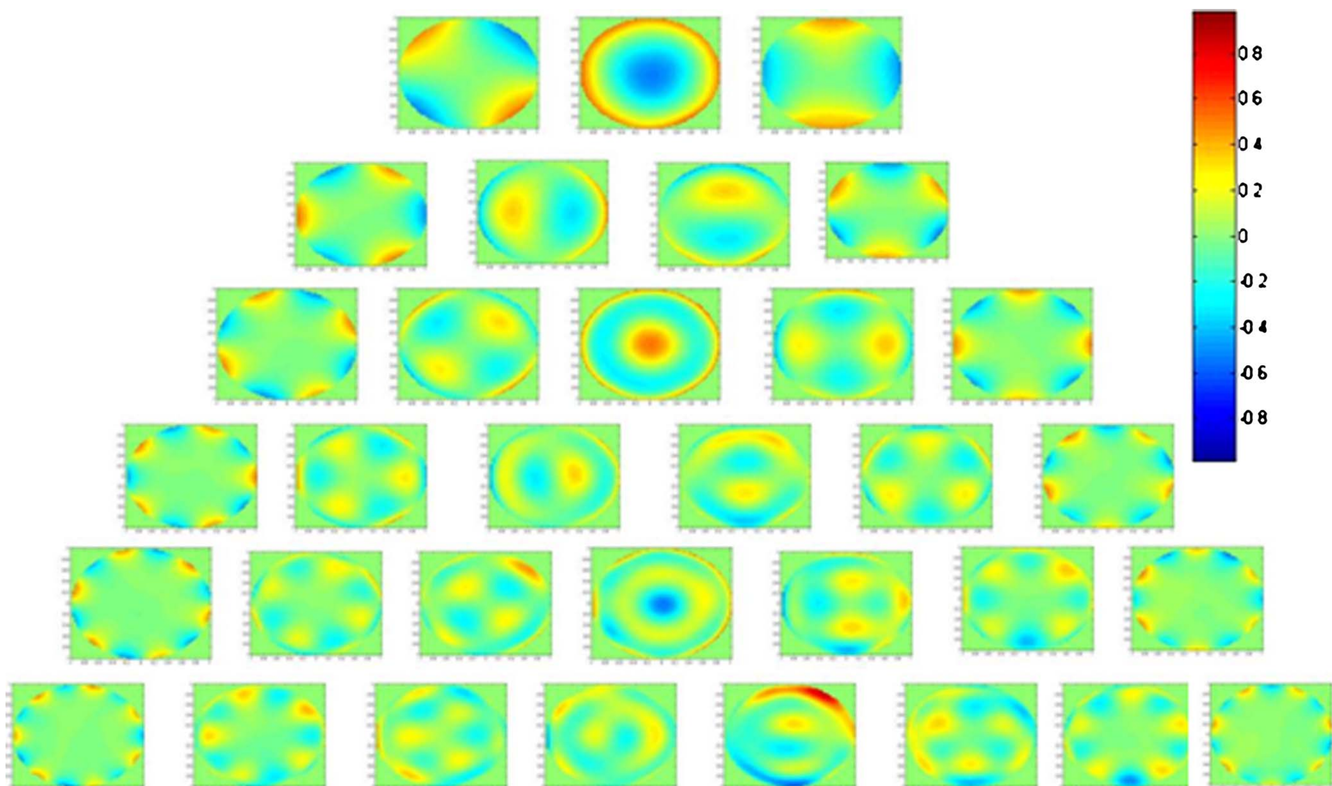

Fig. 2 Zernike shapes made by a 2.5-μm stroke BMC DM, from second to seventh order (orders by row). Measurements made using a Shack–Hartmann wavefront sensor in a closed-loop control system.

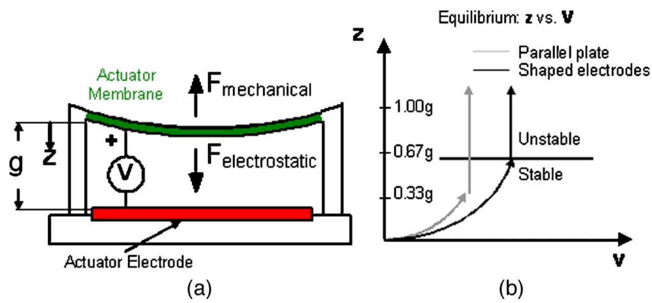

Fig. 3 Schematic of electrostatic actuation of a double cantilever flexure used in the MEMS DM design.

actuator flexure and electrode, a thick sacrificial silicon dioxide film is deposited over the second electrode layer. The thickness of this film is controlled to within 5% to achieve the desired actuator stroke and to maintain operating voltages of <300 V. This film is patterned and etched to provide anchor points for the actuator flexures created by a third structural layer of polysilicon deposited over the sacrificial oxide.

A second sacrificial silicon dioxide layer is deposited over the actuator flexures and chemopolished to remove undesired topography resulting from features etched in the underlying layers. The chemopolish process greatly improves the surface finish of the final poly-silicon mirror layer. This film is then patterned and etched to create mirror post attachment points and to serve as a spacer between the actuator and the mirror, providing sufficient clearance for the mirror membrane for its 4-μm range of motion. A final poly-silicon layer is deposited, patterned, and etched to create the mirror and its post attachments to the center of the actuator flexure. This final polysilicon film is touch polished using CMP to further improve the optical quality of the mirror surface. Pad metal is patterned and deposited onto the bond pads through a liftoff process to facilitate wire bonding of the device. The sacrificial silicon dioxide films are removed with a hydrofluoric acid etch, releasing the structural poly-silicon.

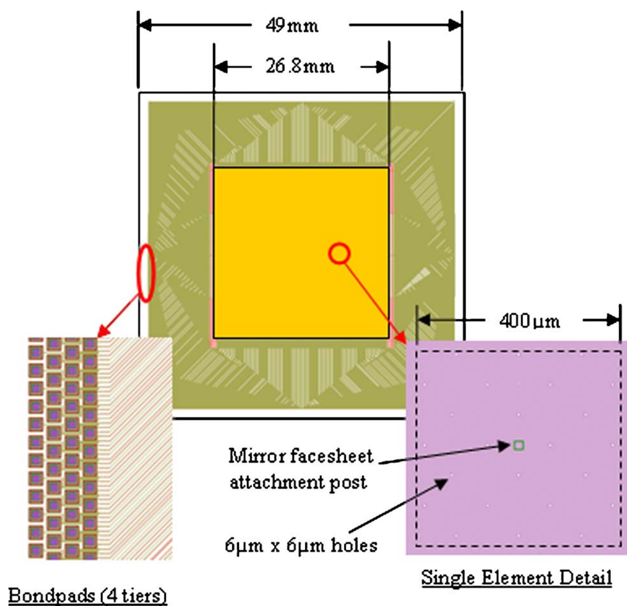

Fig. 4 Layout of 4096 element device.

Table 1 4096 element MEMS deformable mirror requirements.

Description	Requirement
Pixel count	4096 (64×64 array)
Square pitch	400 μm
Stroke	3 μm, after mirror is fully flattened to within 70 (rms)
Fill factor	99%
Active aperture size	19.2 mm (48 actuator diameter at 400 μm pitch)
Pixel surface finish (rms)	<10 nm
Pixel surface finish (P-V)	Three times "Pixel surface finish (rms)"
Bandwidth	5 kHz
Interactuator stroke	1 μm
Yield	100% of actuators on a 48 actuator diameter circular aperture function to spec.
Operating temperature	–5 C

To achieve high reflectivity, a gold coating is applied to the DM, using electron-beam evaporation, after the device has been released. The device is mounted in a ceramic chip carrier to provide structural support and electrical interconnections to the DM actuators. The 4096 electrical interconnections are made using wire bonds between the DM and the chip carrier.

5 DM Surface Figure

The surface figure of the first batch of fabricated devices, measured using a ZYGO NewView 6300 Optical Profiler, is shown in Figs. 6 and 7. A single-element surface finish of <6 nm rms and ~40 nm P-V has been achieved. Most of the P-V error results from the conformal nature of the deposition processes used during fabrication that cause underlying features to print through on the subsequent layers.

The unpowered surface figure of the full DM aperture, shown in Fig. 7, has a radius of curvature of 17 m, resulting in a peak-to-valley bow of ~4 μm in a circular aperture of 25.2 mm. This radius of curvature is attributed mainly to the overall bow of the silicon substrate induced by a mismatch of film stresses on its front and back sides. These stresses result from the fact that all the thin films deposited on the substrate during fabrication are deposited on both front and back sides, but only those on the front side undergo surface micromachining processes, and the sacrificial materials on the front side are largely removed.

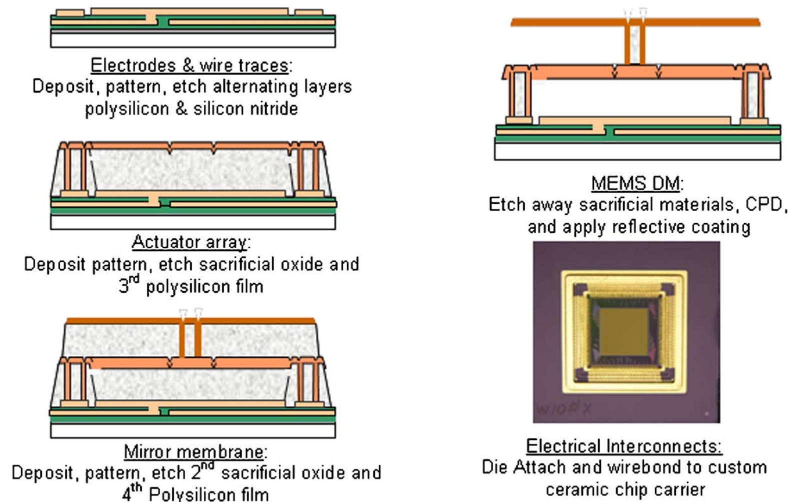

Fig. 5 Fabrication process flow used to BMC's MEMS DMs. A cross section of a single actuator is shown.

Removal of some of the back-side films can mitigate excessive wafer bow, although this process also affects the stresses in the DM actuator flexure and mirror face-sheet films, which in turn affect the electromechanical performance as well as the optical quality of the device. A high-pass filter of 0.83/mm (three DM elements) is applied to the data to investigate nonuniformities in the DM surface figure at spatial frequencies that lie outside of the DM control band (i.e., figure errors at spatial frequencies larger than the pitch of the DM elements of 2.5/mm). As shown in Fig. 7, the P-V surface figure error over all but the very edges of the active aperture is within 30 nm P-V.

6 Device Packaging

A ceramic chip carrier was designed and fabricated to provide electrical interconnections from external drive electronics to each of the 4096 elements of the DM and to provide mechanical support.

The package, shown in Fig. 8, was designed with four tiers of bond fingers around the edge of the central cavity to allow for wire bonding to the DM bond pads, and land grid array pads on the back side to which eight 528 position connectors are attached. High-density interface cables attach directly to the connectors on the back side of the package.

To minimize stresses induced on the DM that would affect the device performance when operating at low temperatures, a die attach process was developed to minimize the stresses on the DM induced by CTE mismatches between the DM (silicon, 2.3 ppm/K) and the ceramic package (alumina, CTE, 7 ppm/K).

Figure 9 shows the results of a study to compare the effects of the modulus of two different die attach adhesives used to bond the silicon MEMS DM die to the ceramic chip carrier. In this study, the surface figure of two 140 element DMs, mounted on alumina chip carriers using epoxies with an elastic modulus of 1 GPa and 6 MPa was measured using an optical surface profiler while the ambient temperature was varied between −30 C and 24 C. Using the more compliant epoxy dramatically reduced the overall stress in the mirror face sheet of the MEMS DM such that the change in surface figure was within 100 nm rms compared to a variation of almost 1 μm rms with the stiffer epoxy. Additional studies will be performed to further decouple the DM from the ceramic package by increasing the bond line thickness.

7 4096 Channel-Drive Electronics

To drive DM at frame rates of >5 kHz, drive electronics have been developed that provide 4096 parallel channels of

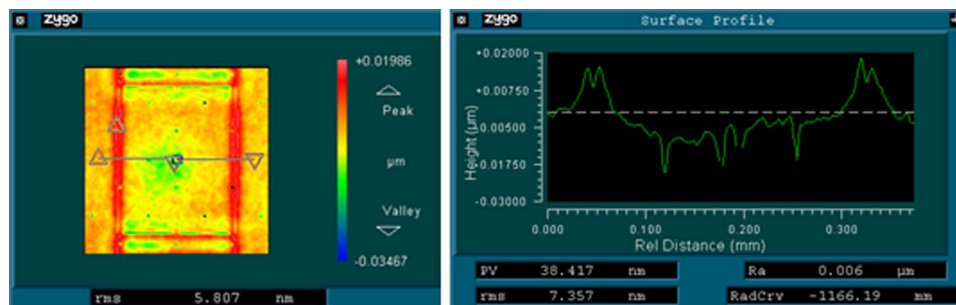

Fig. 6 Single-element surface measurements of MEMS DM with a surface finish of <6 nm rms and 39 nm P-V.

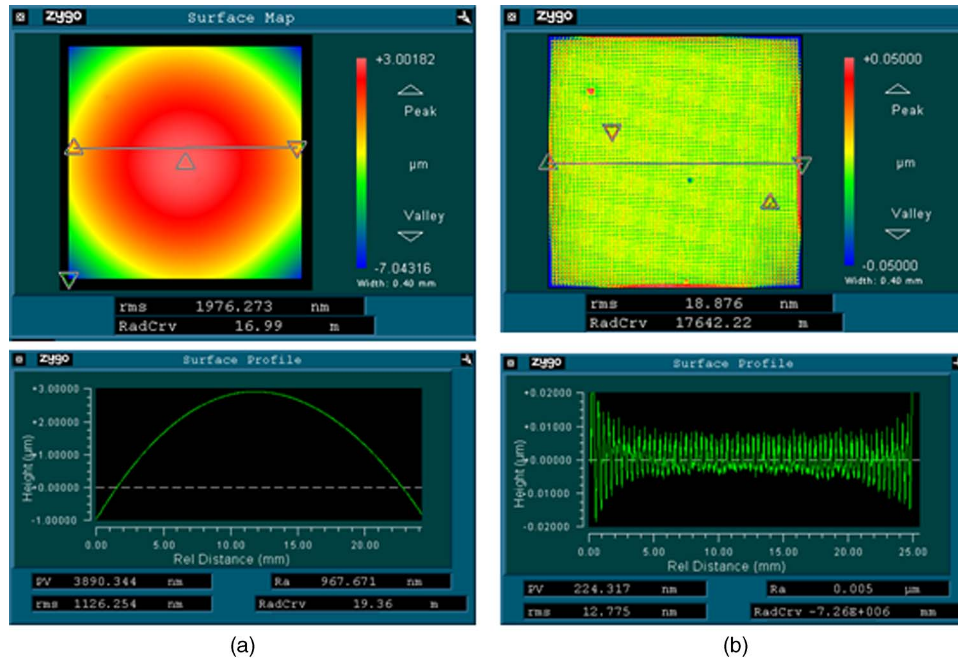

Fig. 7 (a) Surface figure measurements of unpowered 4096 element MEMS showing an overall ROC of 17 m over a 25.2-mm aperture (left). (b) Applying a high-pass filter [λ=1.2 mm (corresponding to three elements)] to the surface data shows the surface figure error that may be outside of the control band (>2.5/mm).

drive voltages up to 285 V with 14-bit resolution. This driver, shown in Fig. 10, uses a 200-MB/s DIO interface and high-density digital-to-analog converters in combination with high-voltage amplifiers to achieve a 45-μs latency (time between first word sent to last DAC written) corresponding to a frame rate of over 22 kHz. Eight flexible cables carrying 512 signals each, carry the high-voltage signals to the DM (see Fig. 10).

8 Device Perfomance

The mechanical stroke (surface) of the DMs was measured by applying a known voltage to a 3×3 region of actuators and performing a differential measurement (subtracting 0 V from test voltage measurement), using a white-light interferometer, to determine the device displacement. The results of three different DMs with different actuator design types are shown in Fig. 11.

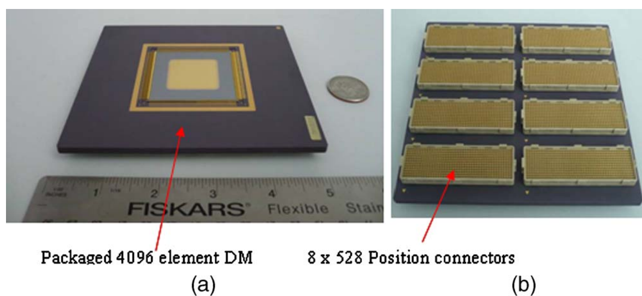

Fig. 8 (a) 4096 element MEMS DM mounted and wirebonded in a ceramic carrier that provides electrical interconnection to each element of the DM. (b) Eight 528 pin connectors are assembled to back side of ceramic carrier.

These results indicate that all the device types can achieve a surface stroke of >3 μm with sufficient margin over the critical deflection (indicated by the last data point on each curve). The operating voltage at 3.5-μm stroke for all devices is between 210 and 260 V.

The device influence function was measured by actuating a single element and measuring the displacement of the neighboring actuator and comparing this to the displacement of the actuated element (see Fig. 12). The measured influence function was <32%, with a variation of <6%.

The interactuator stroke was measured by applying a sine-wave shape, with a period of two actuators, on a subarray of DM elements as shown in Fig. 13. A voltage was

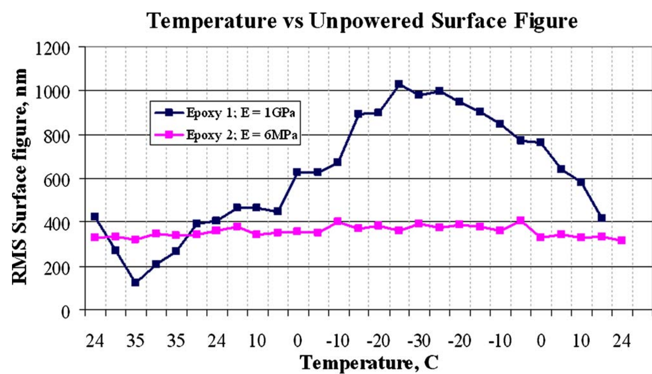

Fig. 9 Comparison of the effect of the elastic modulus of the die attach adhesive on the surface figure of an unpowered, 140-element MEMS DM packaged in an alumina chip carrier as a function of temperature. Using an adhesive with a modulus of 6 MPa minimized the change in DM surface figure between −30 and 24 C.

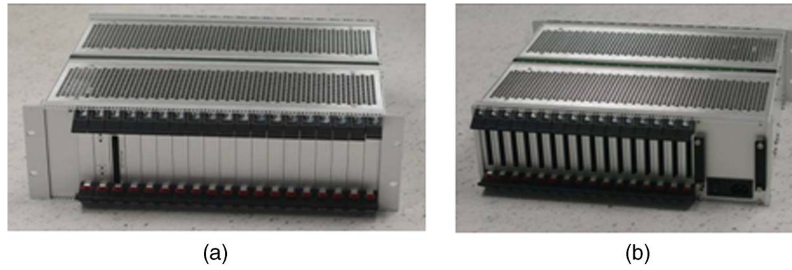

(a) (b)

Fig. 10 (a) Compact 4096 element DM drive electronics (5.25 in. H × 19 in. W × 14 in. D): 200-MB/s DIO input in front of chassis, (b) 4096 high-voltage outputs on rear of chassis.

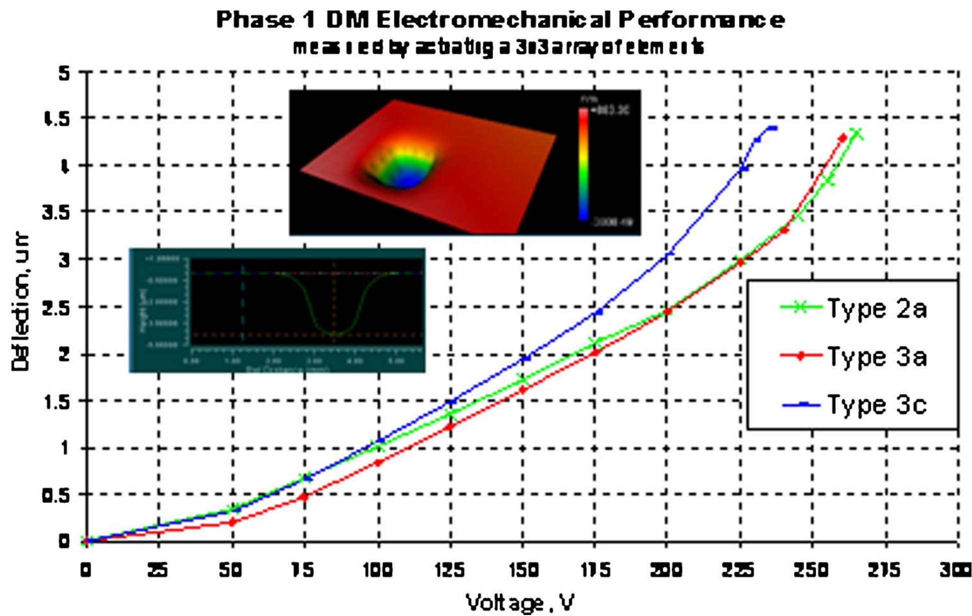

Fig. 11 Voltage versus displacement characteristics of various device types in which a 3 × 3 array is actuated to determine the maximum DM stroke. The small roll-off on some of the devices at maximum displacement is due to the mirror membrane touching down on actuator anchors.

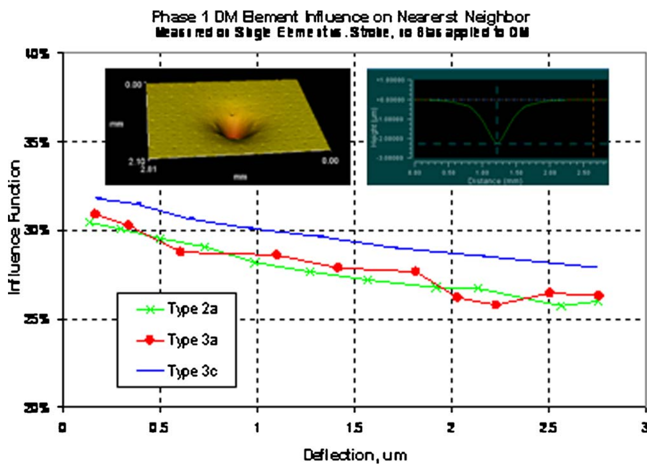

Fig. 12 Influence function of the DMs as a function of DM element displacement. The influence function is tested with no bias applied to the other DM elements.

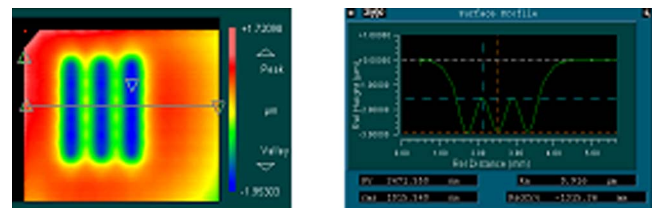

Device Type	Differential displacement, nm	Applied Voltage
Type 2a	1530	240
Type 3a	1770	230
Type 3c	1240	210

Fig. 13 Interactuator stroke measured for the three DM design types is measured to be 1.2–1.7 μm.

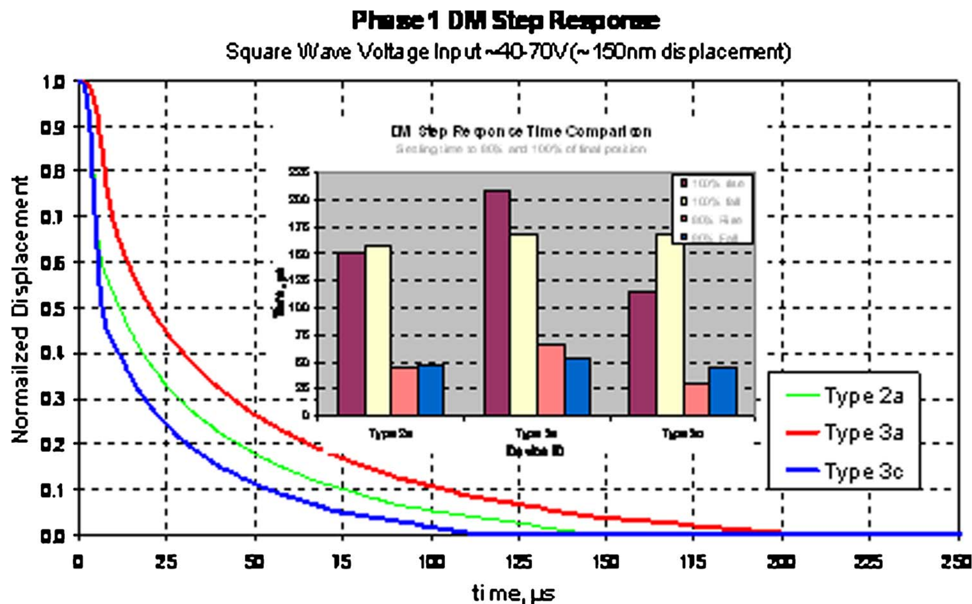

Fig. 14 Normalized dynamic response of each of the three DM design types to a square wave input of ~30 V P-P, corresponding to a displacement of ~150 nm. Each of the three devices settles within 200 μs in response to the voltage step input.

applied to every other row in this subarray to achieve this shape. Each of the three selected DM design types achieved an interactuator stroke of >1 μm.

The settling time of the DMs was measured by providing a step-voltage input, corresponding to ~150-nm displacement (typically 40–70 V step) and measuring the DM's velocity response using a Polytec 3001 laser vibrometer and oscilloscope. The velocity response was integrated to obtain the device displacement responses, which are summarized in Fig. 14. Each of the devices was measured to settle within 200 μs.

9 Conclusion

The results from the first 4096 MEMS deformable mirror devices and its test devices show that the DM designs meet all the functional requirements for the high-contrast imaging applications with exception of the peak-to-valley surface figure and the 3-μm stroke requirement after the DM has been controlled to flat (70 nm rms) due to the bow on the unpowered DM. The source of the single-element peak-to-valley surface figure error, measured to be 39 nm, is the print-through of underlying features and occurs at high frequencies that are outside of the control band of the DM and the associated diffractive light will be filtered out in the intended application. The low-order surface figure error (bow) of the DM surface is not correctable because the peak-to-valley is on the order of the total available stroke on the device. Because this surface error is low order, it can be mitigated using corrective static optics to remove the curvature or a secondary "woofer" DM that would serve to remove the low-order terms. The 4096-element MEMS DM is optimized for the compensation of high-order aberrations at high frame rates that cannot be corrected for by other means.

Acknowledgments

This work has been support by the National Science Foundation Technology Center for Adaptive Optics managed by the University of California at Santa Cruz, and Lawrence Livermore National Laboratories. T. B. acknowledges a financial interest in Boston Micromachines Corporation.

References

1. B. Macintosh, J. Graham, B. Oppenheimer, L. Poyneer, A. Sivaramakrishnan, and J. Veran, "MEMS-based extreme adaptive optics for planet detection," *Proc. SPIE* **6113**, 611308 (2006).
2. J. Evans, K. Morzinski, S. Severson, L. Poyneer, B. Macintosh, D. Dillon, L. Reza, D. Gavel, D. Palmer, S. Olivier, and P. Bierden, "Extreme adaptive optics testbed: performance and characterization of a 1024-MEMS deformable mirror," *Proc. SPIE* **6113**, 61130I (2006).
3. J. A. Perreault, T. G. Bifano, B. M. Levine, and M. Horenstein, "Adaptive optic correction using microelectromechanical deformable mirrors," *Opt. Eng.* **41**(5), 561–566 (2002).
4. T. Bifano, J. Perreault, R. Mali et al., "Microelectromechanical deformable mirrors," *IEEE J. Sel. Top. Quantum Electron.* **5**(1), 83–89 (1999).

Steven A. Cornelissen is vice president of engineering at Boston Micromachines Corporation of Cambridge, Massachusetts. He received his BS in mechanical engineering from San Jose State University and MS in mechanical engineering from Boston University. His research and development work focuses on design and fabrication of optical MEMS devices for wavefront control. Prior to joining Boston Micromachines, he was a research and development engineer at Space Systems/Loral and KLA-Tencor.

Paul A. Bierden received his BS and MS in mechanical engineering from Boston University and has spent over 10 years working with small businesses. Since cofounding Boston Micromachines in 1999, he has led pioneering research efforts in optical MEMS fabrication, system integration, and compact AO while overseeing multiple R&D contracts resulting in over $5M in research funding. Bierden has also spearheaded the commercialization efforts of Boston Micromachines, which has resulted in worldwide sales of BMC's optical MEMS systems.

Thomas G. Bifano is the chief technology officer for Boston Micromachines Corporation. He also serves as the director of Boston University's Photonic's Center and is a professor of the Manufacturing Engineering Department at Boston University, with a joint appointment in Aerospace and Mechanical Engineering. His research focuses on developing useful devices with the aid of novel precision-manufacturing technologies. Currently his active projects center on development of an advanced class of MEMS for optical and biomedical applications. Recent highlights include the development of a MEMS deformable mirror system that improves image resolution in microscopes and telescopes, a MEMS microvalve for ultraprecise flow control, and a spatial light modulator for optical encryption and optical computing. Bifano joined Boston University in 1988. He earned a PhD in mechanical engineering from North Carolina State University in 1988, following his MS and BS in mechanical engineering from Duke University.

Charlie V. Lam: Biography not available.